

Vibration Analysis of a Rotating Nanoplate Using Nonlocal Elasticity Theory

M. Ghadiri^{1,*}, N. Shafiei¹, S. Hossein Alavi²

¹Faculty of Engineering, Department of Mechanics, Imam Khomeini International University, Qazvin, Iran

²School of Mechanical Engineering, Sharif University of Technology, Tehran, Iran

Received 23 February 2017; accepted 19 April 2017

ABSTRACT

The nanostructures under rotation have high promising future to be used in nano-machines, nano-motors and nano-turbines. They are also one of the topics of interests and it is new in designing of rotating nano-systems. In this paper, the scale-dependent vibration analysis of a nanoplate with consideration of the axial force due to the rotation has been investigated. The governing equation and boundary conditions are derived using the Hamilton's principle based on nonlocal elasticity theory. The boundary conditions of the nanoplate are considered as free-free in y direction and two clamped-free (cantilever plate) and clamped-simply (propped cantilever) in x direction. The equations have been solved using differential quadrature method to determine natural frequencies of the rotating nanoplate. For validation, in special cases, it has been shown that the obtained results coincide with literatures. The effects of the nonlocal parameter, aspect ratio, hub radius, angular velocity and different boundary conditions on the first three frequencies have been investigated. Results show that vibration behavior of the rotating nanoplate with cantilever boundary condition is different from other boundary conditions.

© 2017 IAU, Arak Branch. All rights reserved.

Keywords: Rotating nanoplate; Cantilever nanoplate; Propped cantilever nanoplate; Nonlocal elasticity theory; DQM.

1 INTRODUCTION

IN recent years, there has been significant interest in rotating nanomachines which are important in future of nanotechnology. Applications like intelligent drug delivery, DNA nanomachines, programmable chemical synthesis and performing functions similar to the biological molecular motors [1] emphasize this importance. Currently, many researchers take their studies focus on designing nanomachines. For example, [2] designed a nano-turbine composed of carbon nanotube and graphene nano-blades, which can be driven by fluid flow.

The experiments show that the size effects play an important role in mechanical properties [3, 4]. Thus, avoiding these effects may result wrong designs and unacceptable answers. The size effect is not considered in the classical continuum theories so, this theory is not appropriate for micro and nano scales. We are looking for theories that consider the small scale effects. Nonlocal theory of Eringen [5] is one of the best and most well-known continuum mechanics theories that includes small scale effects with good accuracy in nanoscale devices. In nano applications, size effects have been experimentally observed. Classical continuum theories do not interpret such size effects due to lack of material length scale parameters. Hence, size-dependent continuum theories have been developed. The

*Corresponding author. Tel.: +98 28 33901144 ; Fax: +98 28 33780084.
E-mail address: ghadiri@eng.ikiu.ac.ir (M. Ghadiri).

most commonly used theory is the nonlocal elasticity theory introduced by Eringen [5, 6]. In this theory the forces between atoms and the internal length scale are considered in the formulation.

The small scale effect on a large deflection of the cantilever nanobeam under a vertical end loading was investigated by Chen [7]. Moreover, vibration of rotating nanobeams is vastly analyzed. Murmu and Adhikari [8] studied the nonlocal effects on bending vibration of a single-walled carbon nanotube (SWCNT) under pre-stress via nonlocal elasticity. Narendar and Gopalakrishnan [9] investigated the wave dispersion characteristics of a rotating nanotube modeled a SWCNT using spectral analysis. Narendar [10] has modeled a rotating SWCNT as an Euler-Bernoulli beam using the nonlocal/nonclassical continuum mechanics. Clamp-simply supported (propped cantilever [11]) boundary conditions have been considered in [8, 9] and cantilever boundary conditions have also been studied. Challamel and Wang [12] studied bending analysis of small scale rods based on some simplified nonlocal beam theories. Moreover, Lim, Li [13] studied nonlocal stress effect on a nanocantilever considering axial torsion. Moreover, Narendar [14] analyzed flapwise bending free vibration of a nanotube considering transverse shear deformation and rotary inertia based on Eringen's nonlocal theory. Pradhan and Murmu [15] applied DQM method to investigate flapwise bending vibration of a rotating nanocantilever based on nonlocal theory. The nondimensional frequencies of the flapwise bending vibrations of a nonuniform rotating nanocantilever have been calculated by Aranda-Ruiz, Loya [16], they considered time dependent nonlocal boundary conditions. Also recently, Ghadiri and Shafiei [17, 18] investigated linear and nonlinear bending vibration of a rotating nanobeam for various boundary conditions based on nonlocal Eringen's theory.

Kiani [19-21] studied the a small-scale effect on the vibration of thin nanoplates subjected to a moving nanoparticle via nonlocal continuum theory. In-plane and out-of-plane vibrations of a bi-axially-tensioned embedded nanoplate due to the movement of a nanoparticle on its upper surface are investigated via this advanced theory by Kiani [22]. Salehipour, Nahvi [23] presented closed-form solutions for in-plane and out-of-plane free vibration of simply supported functionally graded (FG) rectangular micro/nanoplates. A three-dimensional (3D) elastic plate model capturing the small scale effects is developed for the free vibration of functionally graded nanoplates resting on elastic foundations by Ansari, Shahabodini [24]. It is found from most of the previous studies that, rotation effect on rotary nanoplate has been ignored. As a result, these studies cannot be utilized to study the nanoplate under rotating effect completely. Therefore, there is a strong scientific need to understand the vibration behavior of rotating nanoplates.

Vibration analysis of rotating nanoplates is undoubtedly a prerequisite for designing efficient nanomachines which make use of axial force for their motion. This motivates us to investigate this problem here. So in the present paper, the small scale effects are incorporated into the governing equations and boundary conditions by applying the nonlocal continuum mechanics to the classical plate theory for analyzing vibration behavior of rotating nanoplates under different boundary conditions. Analytical solution is obtained for the natural frequencies of cantilever and propped cantilever boundary conditions and the equation has been solved using differential quadrature method (DQM). The effect of angular velocity, nonlocal parameter, aspect ratio, different boundary conditions and frequency number have been investigated. It is also worth mentioning that, in each vibration mode, the effect of nonlocal parameter is related to the size of the nanoplate. These results are useful to design nano motors, nano rotors and other rotary nano structures.

2 NONLOCAL CONSTITUTIVE RELATIONS

According to Eringen [5] theory, the stress field at point x in an elastic continuum depends not only on the strain field at the point (hyperelastic case) but also on strains at all other points of the body. Eringen [5] also attributed this fact to the atomic theory of lattice dynamics and experimental observations on phonon dispersion. Thus, the nonlocal stress tensor σ at point x is expressed as:

$$\sigma = \int_V K(|x' - x|, \tau) t(x') dx' \quad (1)$$

where $t(x')$ is the classical, macroscopic stress tensor at point x , the kernel function $K(|x' - x|, \tau)$ represents the nonlocal modulus, $|x' - x|$ considered as the distance (in Euclidean norm) and τ is a material constant that depends

on internal and external characteristic lengths (the lattice spacing and wavelength, respectively). The macroscopic stress t at a point x in a Hookean solid is related to the strain ε at the point by the generalized Hooke's law

$$t(x) = C(x) : \varepsilon(x) \tag{2}$$

where C is the fourth-order elasticity tensor and $:$ indicates the 'double-dot product'.

The constitutive Eqs. (1) and (2) together define the nonlocal constitutive behavior of a Hookean solid. Eq. (1) represents the weighted average of the strain field contributions of all points in the body to the stress field at a point. However, the integral constitutive relation in (1) makes the elasticity problems difficult to solve. Though, it is possible [5] to represent the integral constitutive relations in an equivalent differential form as:

$$(1 - \tau^2 l^2 \nabla^2) \sigma = t \tag{3}$$

$$(1 - (e_0 a)^2 \nabla^2) \sigma = t ; \quad \tau = \frac{e_0 a}{l} \tag{4}$$

where e_0 is a material constant, and a and l are the internal and external characteristic lengths, respectively.

3 PROBLEM FORMULATION

Consider an elastic plate of length a in x direction, width b in y direction and thickness h , which is clamped at section ($x = 0$) located at distance r from the axes around which are rotating at constant angular velocity Ω as shown in Fig. 1.

Based on classical plate theory (CPT) The displacement field can be written as:

$$u_x(x, y, t) = u(x, y, t) - z \left(\frac{\partial w}{\partial x} \right) , \quad u_y(x, y, t) = v(x, y, t) - z \left(\frac{\partial w}{\partial y} \right) , \quad u_z(x, y, t) = w(x, y, t) \tag{5}$$

Here u , v and w indicate displacement along x , y and z directions, respectively.

Although the displacement field in Eq. (5) has been derived using the local shear stress–strain constitutive relation, it is assumed that, to be a valid displacement field. The nonzero strains of the refined plane of the theory are

$$\begin{Bmatrix} \varepsilon_{xx} \\ \varepsilon_{yy} \\ \gamma_{xy} \end{Bmatrix} = \begin{Bmatrix} \frac{\partial u}{\partial x} \\ \frac{\partial v}{\partial y} \\ \frac{1}{2} \left(\frac{\partial u}{\partial y} + \frac{\partial v}{\partial x} \right) \end{Bmatrix} - z \begin{Bmatrix} \frac{\partial^2 w}{\partial x^2} \\ \frac{\partial^2 w}{\partial y^2} \\ \frac{\partial^2 w}{\partial x \partial y} \end{Bmatrix} , \quad \varepsilon_{zz} = \varepsilon_{xz} = \varepsilon_{yz} = 0 \tag{6}$$

The displacement field of the refined plate of the theory accommodates a quadratic variation of the transverse shear strain that vanishes on the top and bottom faces, $z = \pm h/2$ of the plate. It can be seen from Eq.(3) that the nonlocal behavior enters the problem through constitutive relations. Principle of virtual work is independent of constitutive relations. So this can be applied to obtain the equations of motion of the nonlocal plates. Using the principle of virtual displacements, following equations can be obtained [25, 26]:

$$\frac{\partial N_{xx}}{\partial x} + \frac{\partial N_{xy}}{\partial y} = I_0 \ddot{u} \tag{7a}$$

$$\frac{\partial N_{xy}}{\partial x} + \frac{\partial N_{yy}}{\partial y} = I_0 \ddot{v} \tag{7b}$$

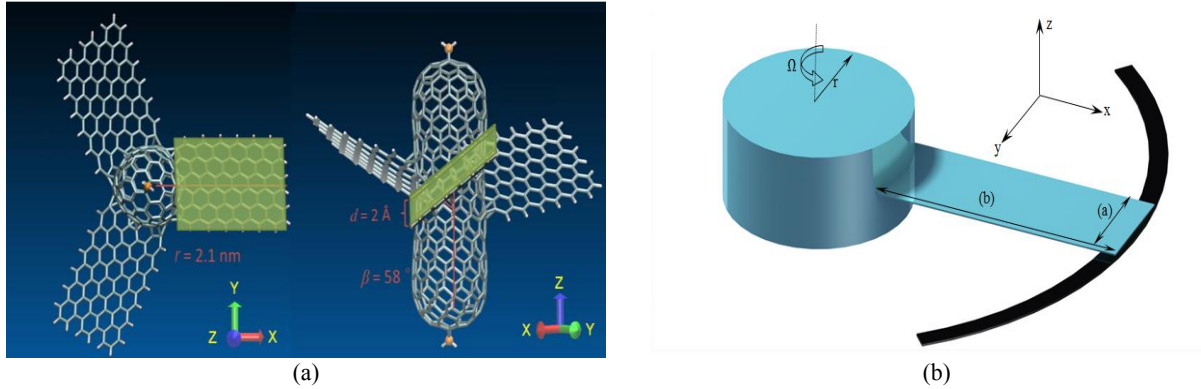


Fig.1

A: Schematic of nano-turbine that introduced by Li et al., [2]. B: Schematic rotating nanoplate that used in this analysis (L: x-direction, b: y-direction).

$$\frac{\partial^2 M_{xx}}{\partial x^2} + 2 \frac{\partial^2 M_{xy}}{\partial x \partial y} + \frac{\partial^2 M_{yy}}{\partial y^2} + q + \frac{\partial}{\partial x} \left(N_{xx} \frac{\partial w}{\partial x} + N_{xy} \frac{\partial w}{\partial y} \right) + \frac{\partial}{\partial y} \left(N_{xy} \frac{\partial w}{\partial x} + N_{yy} \frac{\partial w}{\partial y} \right) = I_0 \ddot{w} - I_2 \left(\frac{\partial^2 \ddot{w}}{\partial x^2} + \frac{\partial^2 \ddot{w}}{\partial y^2} \right) \tag{7c}$$

where, I_0 and I_2 are mass moments of inertia which are defined as follows:

$$I_i = \int_{-h/2}^{h/2} \rho_0(z)^i dz \tag{8}$$

h indicates the thickness of the plate. Although the displacement field in Eq.(5) was obtained using the local shear stress–strain constitutive relation, using (4), the plane stress constitutive relation of a nonlocal plate will be:

$$\begin{Bmatrix} \sigma_{xx} \\ \sigma_{yy} \\ \sigma_{xy} \end{Bmatrix} - (e_0 a)^2 \nabla^2 \begin{Bmatrix} \sigma_{xx} \\ \sigma_{yy} \\ \sigma_{xy} \end{Bmatrix} = \begin{bmatrix} \frac{E_1}{(1-\nu_{12}\nu_{21})} & \frac{\nu_{12}E_2}{(1-\nu_{12}\nu_{21})} & 0 \\ \frac{\nu_{12}E_2}{(1-\nu_{12}\nu_{21})} & \frac{E_2}{(1-\nu_{12}\nu_{21})} & 0 \\ 0 & 0 & G_{12} \end{bmatrix} \begin{Bmatrix} \varepsilon_{xx} \\ \varepsilon_{yy} \\ 2\varepsilon_{xy} \end{Bmatrix} \tag{9}$$

Here E_1 and E_2 are elastic moduli, G_{12} is shear modulus and ν_{12} and ν_{21} represent Poisson’s ratio, respectively. Following stress resultants are used in the present formulation

$$\begin{aligned} N_{xx} &= \int_{-h/2}^{h/2} \sigma_{xx} dz & M_{xx} &= \int_{-h/2}^{h/2} z \sigma_{xx} dz \\ N_{yy} &= \int_{-h/2}^{h/2} \sigma_{yy} dz & M_{yy} &= \int_{-h/2}^{h/2} z \sigma_{yy} dz \\ N_{xy} &= \int_{-h/2}^{h/2} \sigma_{xy} dz & M_{xy} &= \int_{-h/2}^{h/2} z \sigma_{xy} dz \end{aligned} \tag{10}$$

Using strain displacement relation, Eq.(6), stress–strain relation Eq.(9) and stress resultants definition Eq.(10), we can express stress resultants in terms of displacements as follows:

$$\begin{aligned}
 M_{xx} - (e_0a)^2 \nabla^2 M_{xx} &= -D_{11} \frac{\partial^2 w}{\partial x^2} - D_{12} \frac{\partial^2 w}{\partial y^2} \\
 M_{yy} - (e_0a)^2 \nabla^2 M_{yy} &= -D_{12} \frac{\partial^2 w}{\partial x^2} - D_{22} \frac{\partial^2 w}{\partial y^2} \\
 M_{xy} - (e_0a)^2 \nabla^2 M_{xy} &= -2D_{66} \frac{\partial^2 w}{\partial x \partial y}
 \end{aligned}
 \tag{11}$$

where

$$D_{11} = \frac{E_1 h^3}{12(1-\nu_{12}\nu_{21})}, \quad D_{12} = \frac{\nu_{12} E_2 h^3}{12(1-\nu_{12}\nu_{21})}, \quad D_{22} = \frac{E_2 h^3}{12(1-\nu_{12}\nu_{21})}, \quad D_{66} = \frac{G_{12} h^3}{12}
 \tag{12}$$

Using Eqs.(7) and (11), the governing equation in terms of displacement will be:

$$\begin{aligned}
 -D_{11} \frac{\partial^4 w}{\partial x^4} - 2(D_{12} + 2D_{66}) \frac{\partial^4 w}{\partial x^2 \partial y^2} - D_{22} \frac{\partial^4 w}{\partial y^4} + (e_0a)^2 \nabla^2 \left[-q - \frac{\partial}{\partial x} \left(N_{xx} \frac{\partial w}{\partial x} \right) - \frac{\partial}{\partial y} \left(N_{yy} \frac{\partial w}{\partial y} \right) - \frac{\partial}{\partial x} \left(N_{xy} \frac{\partial w}{\partial y} \right) \right] \\
 - \frac{\partial}{\partial y} \left(N_{xy} \frac{\partial w}{\partial x} \right) + I_0 \ddot{w} - I_2 \left(\frac{\partial^2 \ddot{w}}{\partial x^2} + \frac{\partial^2 \ddot{w}}{\partial y^2} \right) \\
 + q + \frac{\partial}{\partial x} \left(N_{xx} \frac{\partial w}{\partial x} \right) + \frac{\partial}{\partial y} \left(N_{yy} \frac{\partial w}{\partial y} \right) + \frac{\partial}{\partial x} \left(N_{xy} \frac{\partial w}{\partial y} \right) + \frac{\partial}{\partial y} \left(N_{xy} \frac{\partial w}{\partial x} \right) = I_0 \ddot{w} - I_2 \left(\frac{\partial^2 \ddot{w}}{\partial x^2} + \frac{\partial^2 \ddot{w}}{\partial y^2} \right)
 \end{aligned}
 \tag{13}$$

Differentiating the (13) with respect to x , considering Young’s modulus and ρ as constants, and setting the external load equal to zero, we can formulate the differential equation that controls the vibrations of the nonlocal classical theory for rotating nanoplate with uniform section.

It is assumed that the plate is free from any in-plane or transverse loadings. Hence we have used airy function, N_{xx} and N_{yy} due to rotation are calculated by follow equation [27]:

$$N_{xy} = q = 0
 \tag{14}$$

$$N_{xx} = \frac{1}{2} \rho h \Omega^2 \left\{ \left[(L^2 - x^2) + 2r(L - x) \right] + 2 \left(\frac{a_{21}}{a_{11}} \right) \left(y^2 - \frac{b^2}{3} \right) \right\}, \quad N_{yy} = \frac{1}{2} \rho h \Omega^2 (b^2 - y^2)
 \tag{15}$$

where Ω indicates the angular velocity and $A = b \times h$, and also, a_{11} and a_{12} are calculated from the following equation:

$$\begin{bmatrix} a_{11} & a_{12} & a_{16} \\ a_{21} & a_{22} & a_{26} \\ a_{16} & a_{62} & a_{66} \end{bmatrix}^{-1} = \begin{bmatrix} \frac{E_1}{(1-\nu_{12}\nu_{21})} & \frac{\nu_{12} E_2}{(1-\nu_{12}\nu_{21})} & 0 \\ \frac{\nu_{12} E_2}{(1-\nu_{12}\nu_{21})} & \frac{E_2}{(1-\nu_{12}\nu_{21})} & 0 \\ 0 & 0 & G_{12} \end{bmatrix}
 \tag{16}$$

Introducing the nondimensional quantities:

$$\begin{aligned}
 w &= LW e^{i\alpha x} & ; & & x &= \xi L \\
 y &= \eta b & ; & & \beta &= \frac{L}{b} \\
 \delta &= \frac{r}{L} & ; & & \mu &= \frac{e_0 a}{L} \\
 \Phi^2 &= \frac{m_0 L^4}{D_{11}} \Omega^2 & ; & & \Psi_{ij} &= \frac{m_0 L^4}{D_{11}} \omega_{ij}^2 \\
 \lambda_1 &= \frac{D_{12} + D_{66}}{D_{11}} & ; & & \lambda_2 &= \frac{D_{22}}{D_{11}} \\
 \bar{I} &= \frac{m_2}{L^2 m_0}
 \end{aligned} \tag{17}$$

Using Eq.(16), we can express the governing equation (CPT) in terms of displacement as follows:

$$\begin{aligned}
 & \frac{\partial^4 W}{\partial \xi^4} + 2\beta^2 \lambda_1 \frac{\partial^4 W}{\partial \xi^2 \partial \eta^2} + \beta^4 \lambda_2 \frac{\partial^4 W}{\partial \eta^4} - (-\Phi^2 [\xi + \delta]) \frac{\partial W}{\partial \xi} - \beta^2 \left(-\frac{\Phi^2}{\beta^2} \eta \right) \frac{\partial W}{\partial \eta} \\
 & - \beta^2 \left(\frac{\Phi^2}{2\beta^2} (1 - \eta^2) \right) \frac{\partial^2 W}{\partial \eta^2} - \left(\frac{1}{2} \Phi^2 \left[(1 - \xi^2) + 2\delta(1 - \xi) + 2 \left(\frac{a_{21}}{a_{11}} \right) \left(\eta^2 - \frac{1}{3} \right) / \beta^2 \right] \right) \frac{\partial^2 W}{\partial \xi^2} \\
 & \left[\begin{aligned}
 & (-\Phi^2 [\xi + \delta]) \frac{\partial^3 W}{\partial \xi^3} + (-\Phi^2) \frac{\partial^3 W}{\partial \xi^2} \\
 & + \left(\frac{1}{2} \Phi^2 \left[(1 - \xi^2) + 2\delta(1 - \xi) + 2 \left(\frac{a_{21}}{a_{11}} \right) \left(\eta^2 - \frac{1}{3} \right) / \beta^2 \right] \right) \frac{\partial^4 W}{\partial \xi^4} \\
 & + \mu^2 + \beta^2 \left((-\Phi^2 [\xi + \delta]) \frac{\partial^3 W}{\partial \xi \partial \eta^2} + \left(2\Phi^2 \left(\frac{a_{21}}{a_{11}} \right) / \beta^2 \right) \frac{\partial^2 W}{\partial \xi^2} \right. \\
 & \left. + \left(\frac{1}{2} \Phi^2 \left[(1 - \xi^2) + 2\delta(1 - \xi) + 2 \left(\frac{a_{21}}{a_{11}} \right) \left(\eta^2 - \frac{1}{3} \right) / \beta^2 \right] \right) \frac{\partial^4 W}{\partial \xi^2 \partial \eta^2} \right) \\
 & \beta^2 \left(\left(-\frac{\Phi^2}{\beta^2} \eta \right) \frac{\partial^3 W}{\partial \xi^2 \partial \eta} + \left(\frac{\Phi^2}{2\beta^2} (1 - \eta^2) \right) \frac{\partial^4 W}{\partial \xi^2 \partial \eta^2} \right) \\
 & + \beta^4 \left(\left(-\frac{\Phi^2}{\beta^2} \eta \right) \frac{\partial^3 W}{\partial \eta^3} + \left(-\frac{\Phi^2}{\beta^2} \right) \frac{\partial^2 W}{\partial \eta^2} + \left(\frac{\Phi^2}{2\beta^2} (1 - \eta^2) \right) \frac{\partial^4 W}{\partial \eta^4} \right)
 \end{aligned} \right] \\
 & = \Psi^4 \left[\mu^2 \bar{I} \left(\frac{\partial^4 W}{\partial \xi^4} + 2\beta^2 \frac{\partial^4 W}{\partial \xi^2 \partial \eta^2} + \beta^4 \frac{\partial^4 W}{\partial \eta^4} \right) - \mu^2 \left(\frac{\partial^2 W}{\partial \xi^2} + \beta^2 \frac{\partial^2 W}{\partial \eta^2} \right) - \bar{I} \left(\frac{\partial^2 W}{\partial \xi^2} + \beta^2 \frac{\partial^2 W}{\partial \eta^2} \right) + W \right]
 \end{aligned} \tag{18}$$

The corresponding boundary conditions are defined as follows:

For the cantilever (CFFF) boundary condition:

Clamped at $x = 0$ and free at other edges ($x = L, y = 0$ and b).

$$w(0, y) = 0 \quad \frac{\partial w(0, y)}{\partial x} = 0 \tag{19}$$

$$V(x, 0) = \frac{\partial M_{yy}(x, 0)}{\partial y} + \frac{\partial M_{xy}(x, 0)}{\partial x} = 0 \quad M_{yy}(x, 0) = 0 \quad (20)$$

$$V(L, y) = \frac{\partial M_{xx}(L, y)}{\partial x} + \frac{\partial M_{xy}(L, y)}{\partial y} = 0 \quad M_{xx}(L, y) = 0 \quad (21)$$

$$V(x, b) = \frac{\partial M_{yy}(x, b)}{\partial y} + \frac{\partial M_{xy}(x, b)}{\partial x} = 0 \quad M_{yy}(x, b) = 0 \quad (22)$$

For propped cantilever (CSFF) boundary condition:
 Clamped at $x = 0$, simply supported at $x = L$ and Free at $y = 0$ and b .

$$w(0, y) = 0 \quad \frac{\partial w(0, y)}{\partial x} = 0 \quad (23)$$

$$V(x, 0) = \frac{\partial M_{yy}(x, 0)}{\partial y} + \frac{\partial M_{xy}(x, 0)}{\partial x} = 0 \quad M_{yy}(x, 0) = 0 \quad (24)$$

$$w(L, y) = 0 \quad M_{xx}(L, y) = 0 \quad (25)$$

$$V(x, b) = \frac{\partial M_{yy}(x, b)}{\partial y} + \frac{\partial M_{xy}(x, b)}{\partial x} = 0 \quad M_{yy}(x, b) = 0 \quad (26)$$

4 SOLUTION PROCEDURE

4.1 Differential quadrature method

The essence of the differential quadrature method lies in partial derivative approximation of a function with respect to a coordinate at a discrete point like the weighted linear sum of the function values at all discrete points along the coordinate.

In addition, in a large number of practical applications where only reasonably accurate solutions at few specified physical coordinates are of interest, conventional numerical methods such as finite element or finite difference method require a large number of grid points and a large capacity of processor. Among various numerical methods, the finite element method is, by far, the most effective and widely used one. Furthermore, the finite element method is still an effective method especially for systems with complex geometries and load conditions or devices with nonlinear behavior. In searching for a more efficient numerical method that requires fewer grid points but yet results acceptable accuracy, the method of differential quadrature (DQ) which was developed by Shu and Richards [28] will appear.

The DQ method, akin to the conventional integral quadrature method, approximates the derivative of a function at each point by a linear summation of all the functional values along a mesh line. The key procedure in the DQ lies in determination of the weighting coefficients. Initially, Bellman and his associates proposed two methods to compute the weighting coefficients for the first order derivative. As a result, the DQ method has emerged as a powerful numerical discretization tool in the past decade. Compared to the conventional low order finite difference and finite element methods, the DQ method can obtain very accurate numerical results using a considerably smaller number of grid points and hence making less effort. So far, the DQ method has been efficiently employed in a variety of problems in engineering and physical sciences Shu and Richards [28].

Let $\frac{\partial^r f}{\partial x^r}$ be the r -th derivative of a function $f(x)$ which can be expressed as a linear sum of the function values

$$\left. \frac{\partial^r f(x)}{\partial x^r} \right|_{x=x_p} = \sum_{j=1}^n C_{ij}^{(r)} f(x_j) \quad (27)$$

where n is the number of total discrete grid points used in the approximation process and $C_{pq}^{(r)}$ are weighting coefficients. The weighting coefficients of the first derivative are determined by

$$C_{ij}^{(1)} = \frac{M(x_i)}{(x_i - x_j)M(x_j)} \quad i, j = 1, 2, \dots, n \text{ and } i \neq j$$

$$C_{ij}^{(1)} = - \sum_{j=1, j \neq i}^n C_{ij}^{(1)} \quad i = j \quad (28)$$

where

$$M(x_i) = \prod_{j=1, j \neq i}^n (x_i - x_j) \quad (29)$$

In order to evaluate the weighting coefficients of the higher-order derivatives, recurrence relations are obtained as:

$$C_{ij}^{(r)} = r \left[C_{ij}^{(r-1)} C_{ij}^{(1)} - \frac{C_{ij}^{(r-1)}}{(\xi_i - \xi_j)} \right] \quad i, j = 1, 2, \dots, n, i \neq j \text{ and } 2 \leq r \leq n-1$$

$$\bar{C}_{ij}^{(r)} = r \left[\bar{C}_{ij}^{(r-1)} \bar{C}_{ij}^{(1)} - \frac{\bar{C}_{ij}^{(r-1)}}{(\eta_i - \eta_j)} \right] \quad i, j = 1, 2, \dots, n, i \neq j \text{ and } 2 \leq r \leq n-1 \quad (30)$$

$$C_{ii}^{(r)} = - \sum_{j=1, j \neq i}^n C_{ij}^{(r)} \quad i, j = 1, 2, \dots, n \quad \text{and } 1 \leq r \leq n-1$$

$$\bar{C}_{ii}^{(r)} = - \sum_{j=1, j \neq i}^n \bar{C}_{ij}^{(r)} \quad i, j = 1, 2, \dots, n \quad \text{and } 1 \leq r \leq n-1$$

The simplest choice of grid points is equally spaced points in the direction of the coordinate axes of the computational domain. It has been demonstrated that nonuniform grid points show better results with the same number of equally spaced grid points. In this paper, we chose these set of grid points in terms of natural coordinate directions x and y as:

$$\xi_i = \eta_i = \frac{1}{2} \left(1 - \cos \left(\frac{(2i-1)\pi}{2(N-2)} \right) \right) \quad i = 1, 2, 3, \dots, n \quad (31)$$

4.2 DQ analog of field equations

Substituting Eq.(27) into(18), governing equation of nanoplate rotation will be:

$$\begin{aligned}
 & \sum_{k=1}^{n_i} C_{i,k}^{(4)} W_{k,j} + 2\beta^2 \lambda_1 \sum_{k=1}^{n_i} \sum_{k=2}^{n_j} C_{i,k}^{(2)} \bar{C}_{i,k}^{(2)} W_{k_1,k_2} + \beta^4 \lambda_2 \sum_{k=2}^{n_j} \bar{C}_{i,k}^{(4)} W_{i,k} + (\Phi^2 [\xi + \delta]) \sum_{k=1}^{n_i} C_{i,k}^{(1)} W_{k,j} \\
 & - \left(\frac{1}{2} \Phi^2 \left[(1 - \xi^2) + 2\delta(1 - \xi) + 2 \left(\frac{a_{21}}{a_{11}} \right) \left(\eta^2 - \frac{1}{3} \right) / \beta^2 \right] \right) \sum_{k=1}^{n_i} C_{i,k}^{(4)} W_{k,j} + \beta^2 \left(\frac{\Phi^2}{\beta^2} \eta \cos^2 \theta \right) \sum_{k=2}^{n_j} \bar{C}_{i,k}^{(1)} W_{i,k} \\
 & - \beta^2 \left(\frac{\Phi^2}{2\beta^2} (1 - \eta^2) \right) \sum_{k=2}^{n_j} \bar{C}_{i,k}^{(2)} W_{i,k} \\
 & + \mu^2 \left[\begin{aligned}
 & - (\Phi^2 [\xi + \delta]) \sum_{k=1}^{n_i} C_{i,k}^{(3)} W_{k,j} - (\Phi^2) \sum_{k=1}^{n_i} C_{i,k}^{(2)} W_{k,j} + \left(\frac{1}{2} \Phi^2 \left[(1 - \xi^2) + 2\delta(1 - \xi) \right. \right. \\
 & \left. \left. + 2 \left(\frac{a_{21}}{a_{11}} \right) \left(\eta^2 - \frac{1}{3} \right) / \beta^2 \right] \right) \sum_{k=1}^{n_i} C_{i,k}^{(4)} W_{k,j} \\
 & + \beta^2 \left(- (\Phi^2 [\xi + \delta]) \sum_{k=1}^{n_i} \sum_{k=2}^{n_j} C_{i,k}^{(1)} \bar{C}_{i,k}^{(2)} W_{k_1,k_2} + \left(\Phi^2 2 \left(\frac{a_{21}}{a_{11}} \right) / \beta^2 \right) \sum_{k=1}^{n_i} C_{i,k}^{(2)} W_{k,j} \right) \\
 & + \left(\frac{1}{2} \Phi^2 \left[(1 - \xi^2) + 2\delta(1 - \xi) \right. \right. \\
 & \left. \left. + 2 \left(\frac{a_{21}}{a_{11}} \right) \left(\eta^2 - \frac{1}{3} \right) / \beta^2 \right] \right) \sum_{k=1}^{n_i} \sum_{k=2}^{n_j} C_{i,k}^{(2)} \bar{C}_{i,k}^{(2)} W_{k_1,k_2} \\
 & \beta^2 \left(- \left(\frac{\Phi^2}{\beta^2} \eta \right) \sum_{k=1}^{n_i} \sum_{k=2}^{n_j} C_{i,k}^{(2)} \bar{C}_{i,k}^{(1)} W_{k_1,k_2} \right. \\
 & \left. + \left(\frac{\Phi^2}{2\beta^2} (1 - \eta^2) \right) \sum_{k=1}^{n_i} \sum_{k=2}^{n_j} C_{i,k}^{(2)} \bar{C}_{i,k}^{(2)} W_{k_1,k_2} \right) \\
 & + \beta^4 \left(- \left(\frac{\Phi^2}{\beta^2} \eta \right) \sum_{k=2}^{n_j} \bar{C}_{i,k}^{(3)} W_{i,k} - \left(\frac{\Phi^2}{\beta^2} \right) \sum_{k=2}^{n_j} \bar{C}_{i,k}^{(2)} W_{i,k} \right) \\
 & \left. + \left(\frac{\Phi^2}{2\beta^2} (1 - \eta^2) \right) \sum_{k=2}^{n_j} \bar{C}_{i,k}^{(4)} W_{i,k} \right) \\
 & = \Psi^4 \left[\begin{aligned}
 & \mu^2 \bar{I} \left(\sum_{k=1}^{n_i} C_{i,k}^{(4)} W_{k,j} + 2\beta^2 \sum_{k=1}^{n_i} \sum_{k=2}^{n_j} C_{i,k}^{(2)} \bar{C}_{i,k}^{(2)} W_{k_1,k_2} + \beta^4 \sum_{k=2}^{n_j} \bar{C}_{i,k}^{(4)} W_{i,k} \right) \\
 & - \mu^2 \left(\sum_{k=1}^{n_i} C_{i,k}^{(2)} W_{k,j} + \beta^2 \sum_{k=2}^{n_j} \bar{C}_{i,k}^{(2)} W_{i,k} \right) - \bar{I} \left(\sum_{k=1}^{n_i} C_{i,k}^{(2)} W_{k,j} + \beta^2 \sum_{k=2}^{n_j} \bar{C}_{i,k}^{(2)} W_{i,k} \right) + W_{ij} \\
 \end{aligned} \right] \tag{32}
 \end{aligned}$$

where $C_{ij}^{(r)}$ and $\bar{C}_{ij}^{(r)}$ are the weighting coefficients associated with the r th-order derivatives in x - and y -directions, respectively. n_i and n_j are also the numbers of total discrete grid points along x and y directions, respectively. The grid points are chosen based on well-established Chebyshev-Gauss-Lobatto Points [28] whose relation is visible in Eq.(31). Finally, by using Eq.(31) with boundary conditions (Eqs. (18)-(25)) and using eigenvalue equation in the form of (33), the overall problem will be solved.

$$\begin{bmatrix} [A_{bb}] & [A_{bi}] \\ [A_{ib}] & [A_{ii}] \end{bmatrix} \begin{Bmatrix} W_b \\ W_i \end{Bmatrix} = \Psi_{ij}^4 \begin{bmatrix} 0 & 0 \\ [B_{ib}] & [B_{ii}] \end{bmatrix} \begin{Bmatrix} W_b \\ W_i \end{Bmatrix} \tag{33}$$

5 RESULTS AND DISCUSSION

In this article the small-scale effects on the vibration response of rotating cantilever and propped cantilever nanoplates are shown with respect to angular velocity of rotation, hub radius and aspect ratio. The boundary conditions of nanoplate are considered as free-free in y direction and two clamped-free (cantilever plate) and clamped-simply (propped cantilever) types in x direction. As DQ results are sensitive to low grid points, a convergence test is performed to determine the minimum number of grid points required to obtain stable and accurate results. As presented in Table 1. solution is in good convergence. It can be seen clearly that $N_x = N_y = 15$ are sufficient to obtain the accurate solutions for the present analysis. For validation of results, material properties of nanoplate are assumed isotropic according to Ref. [29-32]. So, the Young's moduli, Poisson's ratios, density and thickness are, respectively:

$$E = 1.06(TPa), \nu = 0.25, \rho = 2250(kg/m^3), h = 0.34nm$$

Properties of the orthotropic nanoplate in this paper are considered identical to [30] as:

$$E_1 = 1756Gpa, E_2 = 1588Gpa, \nu_{12} = 0.3, \nu_{21} = 0.27, \rho = 2300kg/m^3$$

Since the vibration analysis of a propped cantilever nanoplate has not been investigated before, our results have been compared with a nanoplate with SSSS (all edges simply supported), SCSC and cantilever plate (CFFF) based on classical plate theory. They have been listed in Table 2, 3 and 4, respectively. It is observed that the present results are in good agreement with the available results in the literature.

Table 1

Convergence of nondimensional fundamental frequency (ψ) for the orthotropic cantilever and the propped cantilever nanoplate, $\delta = 1, a = 10h, \gamma = 0$.

	Number of grid point	$\mu = 0$	$\mu = 0.1$	$\mu = 0.2$	$\mu = 0.3$	$\mu = 0.4$	$\mu = 0.5$
Cantilever	5	2.181	2.1943	2.2369	2.3182	2.4628	2.7452
	7	1.8596	1.8622	1.8702	1.884	1.9047	1.9345
	9	1.8191	1.8224	1.8326	1.8511	1.8807	1.928
	11	1.8596	1.8622	1.8702	1.884	1.9047	1.9345
	13	1.8596	1.8622	1.8702	1.884	1.9047	1.9345
	15	1.8596	1.8622	1.8702	1.884	1.9047	1.9345
	17	1.8596	1.8622	1.8702	1.884	1.9047	1.9345
	19	1.8596	1.8622	1.8702	1.884	1.9047	1.9345
	21	1.8596	1.8622	1.8702	1.884	1.9047	1.9345
	23	1.8596	1.8622	1.8702	1.884	1.9047	1.9345
	25	1.8596	1.8622	1.8702	1.884	1.9047	1.9345
Propped Cantilever	5	4.3751	4.1712	3.7558	3.3547	3.0268	2.7666
	7	4.23614	4.0991	3.7838	3.4379	3.1313	2.876
	9	4.0578	3.9442	3.6747	3.3674	3.0862	2.8471
	11	3.9305	3.8345	3.6000	3.3232	3.0620	2.8349
	13	4.2314	4.0991	3.7838	3.4379	3.1313	2.8764
	15	4.2361	4.0991	3.7838	3.4379	3.1313	2.8764
	17	4.2361	4.0991	3.7838	3.4379	3.1313	2.8764
	19	4.2361	4.0991	3.7838	3.4379	3.1313	2.8764
	21	4.2361	4.0991	3.7838	3.4379	3.1313	2.8764
	23	4.2361	4.0991	3.7838	3.4379	3.1313	2.8764
	25	4.2361	4.0991	3.7838	3.4379	3.1313	2.8764

Table 2

Comparison of results for vibration of the isotropic nanoplate with simply supported edges.

Nonlocal parameter μ	Frequency ratio			Natural frequency (THz)	
	[29]	[29]	present	present	[31]
0	1	1	1	0.069056	0.0691217
1	0.9139	0.9139	0.9139	0.06308	0.0631678
2	0.8467	0.8468	0.8467	0.058472	0.0585276
3	0.7925	0.7926	0.7925	0.054728	0.0547796

Table 3

Comparison of results for vibration of the orthotropic nanoplate with SCSC boundary condition.

	$e_0a = 0$	$e_0a = 0.5(nm)$	$e_0a = 1(nm)$	$e_0a = 1.5(nm)$	$e_0a = 2(nm)$
[31]	27.9208	27.1853	25.2818	22.835	20.3555
[30]	27.9207	27.1851	25.2813	22.8341	20.3543
Present	27.9208	27.185	25.2815	22.834	20.3545

Table 4

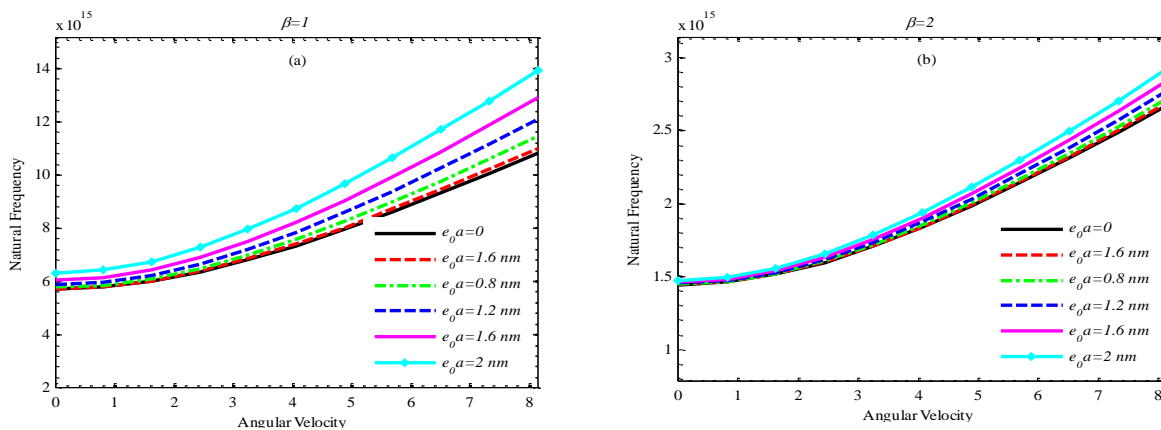
Comparison of results for fundamental frequency of the classical plate with cantilever boundary condition.

	mode number=1	mode number=2	mode number=3	mode number=4
Experimental [30]	3.494	8.547	21.44	27.46
[29]	3.41	8.28	21.45	26.67
Present (Ψ^2)	3.4583	8.885	21.4397	27.4498

To study the vibration characteristics of the rotating rectangular nanoplate with CFFF and CSFF boundary conditions, first four nondimensional frequencies of cantilever and propped cantilever boundary condition are obtained for two aspect ratios.

5.1 Results for cantilever boundary condition

Fundamental frequency of the orthotropic rectangular nanoplate in different nonlocal parameters with respect to angular velocity in four values of aspect ratio i.e. ' $\beta = 1-8$ ' is shown in Fig.2. The nonlocal parameter, width of the square nanoplate and hub radius (δ), are assumed $0-2nm, 4(nm)$ and 0 respectively. It is seen that in the cantilever nanoplate, fundamental frequency decreases while the aspect ratio increases. In this special boundary condition, the fundamental frequency also increases with increase of the nonlocal parameter (like cantilever nanobeam [16]). Furthermore, it is observed that fundamental frequency increases with increase of the angular velocity.



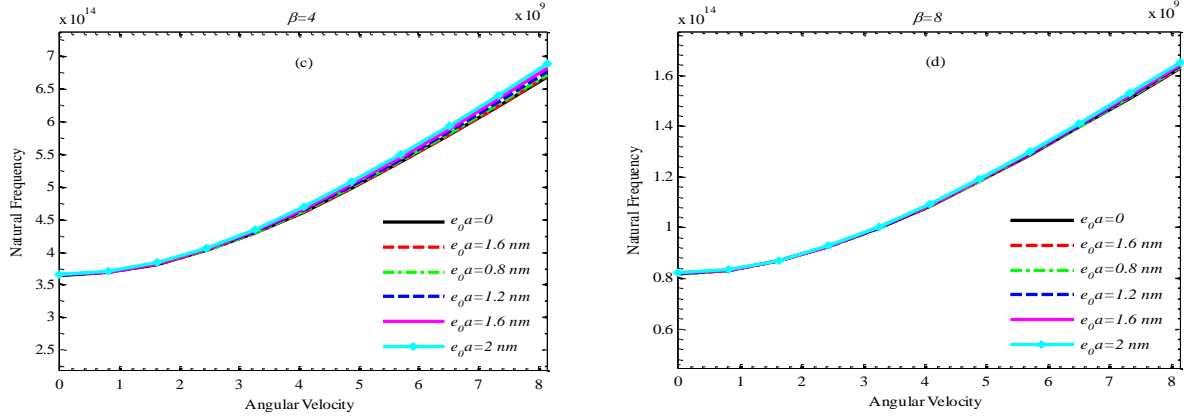


Fig.2

The fundamental frequency of the cantilever nanoplate with respect to dimensional angular velocity, for different nonlocal parameters and aspect ratios, $\delta = 0, L/h = 20$.

Fig.3 indicates the variation of the second frequency of the nanoplate with respect to angular velocity. As it can be seen, the second frequency decreases with increasing the aspect ratio. In addition, with increasing the angular velocity, the second frequency will be increased. It is observed that, the behavior of second frequency with respect to nonlocal parameter depends on aspect ratio (β) and angular velocity, so that, in low angular velocities, the second frequency decreases with increasing the nonlocal parameter.

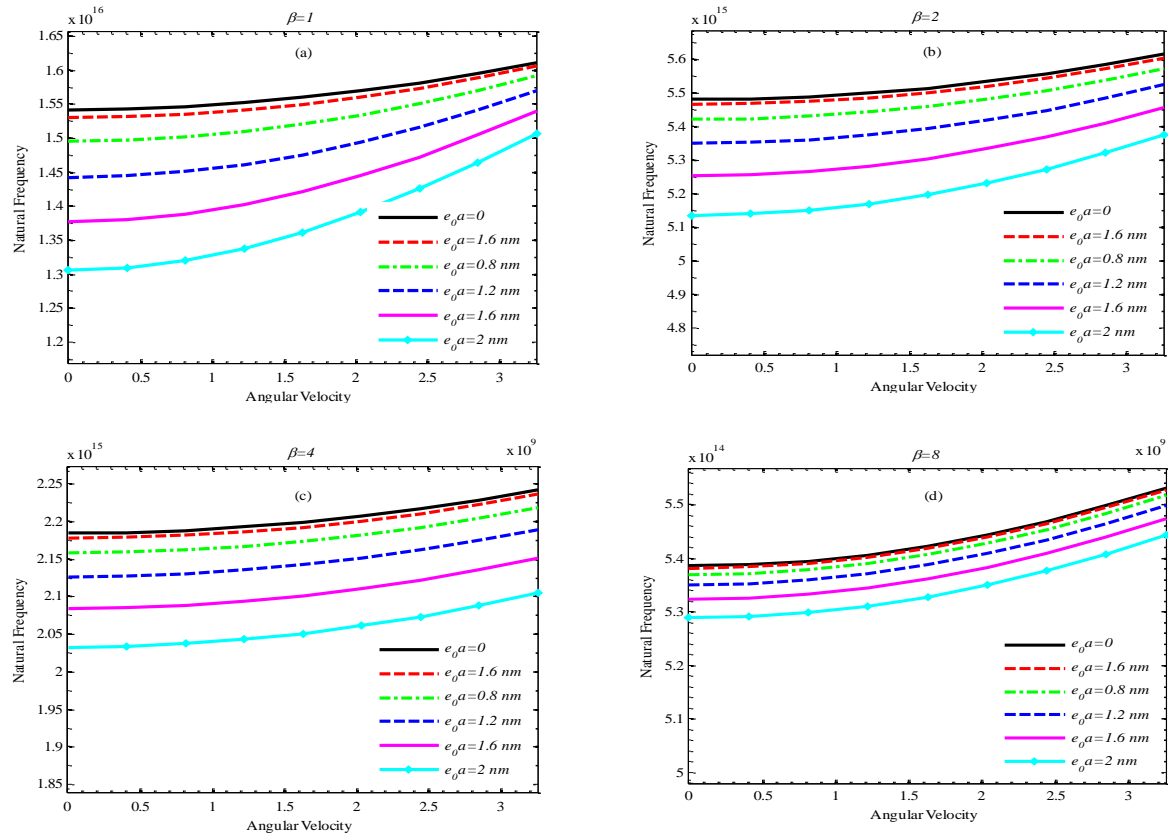


Fig.3

The second frequency of the cantilever nanoplate with respect to angular velocity, for different nonlocal parameters and aspect ratios.

The behavior of the third frequency of the nanoplate with respect to angular velocity is shown in Fig.4. As can be seen, the third frequency decreases with increasing the aspect ratio. In addition, with increasing the angular velocity, the third frequency will be increased. The behavior of the third frequency with respect to the nonlocal parameter depends on the aspect ratio and the angular velocity.

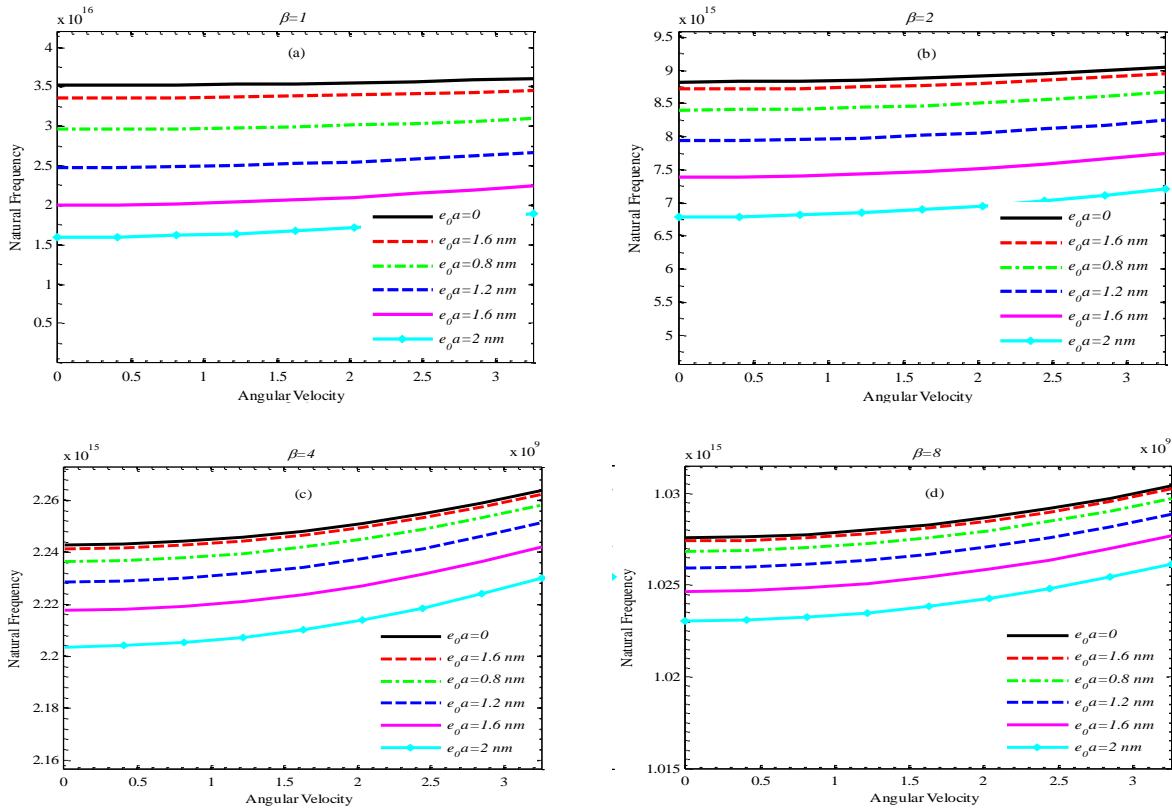
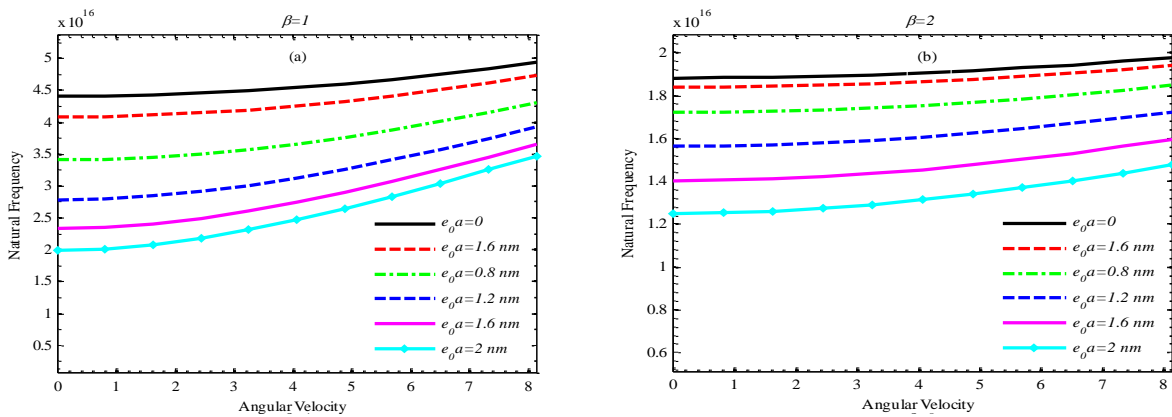


Fig.4 The third frequency of the cantilever nanoplate with respect to angular velocity, for different nonlocal parameters and aspect ratios.

Finally, the fourth frequency of the nanoplate with respect to the angular velocity is shown in Fig.5. As can be seen, the fourth frequency decreases with increasing the aspect ratio. With increasing the angular velocity, the fourth frequency will be also increased. In addition, with increasing the nonlocal parameter, decrease of the fourth fundamental frequency will be observed.



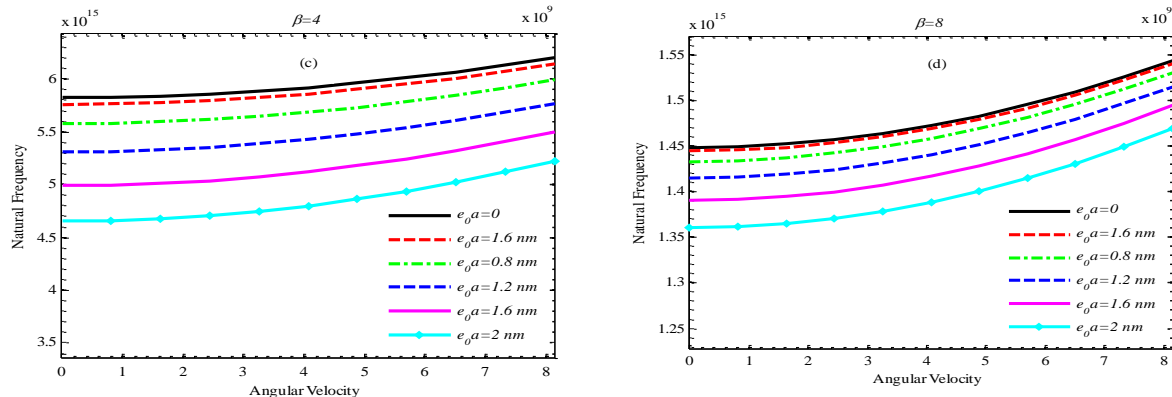


Fig.5 The fourth frequency of the cantilever nanoplate with respect to angular velocity, for different nonlocal parameters and aspect ratios.

5.2 Results for the propped cantilever boundary condition

The fundamental frequency of the orthotropic rectangular propped cantilever nanoplate (CSFF boundary condition) for different nonlocal parameters with respect to the angular velocity for different nonlocal parameters is shown in Fig.6. The nonlocal parameter, the length of the square nanoplate and the hub radius (δ) are considered 0-2 nm, 20h and 0 respectively. It is seen that in CSFF boundary condition, the fundamental frequency increases while angular velocity increases. In this boundary condition, the fundamental frequency also decreases with increase of the nonlocal parameter.

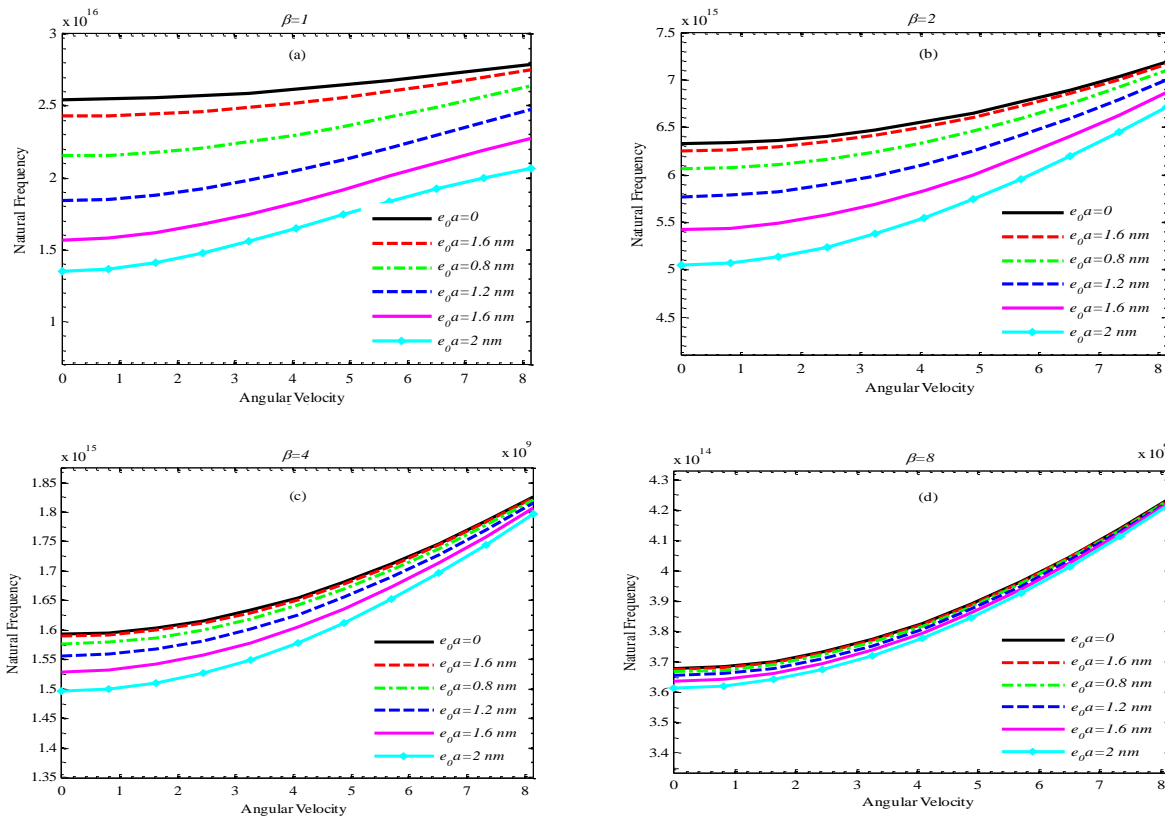


Fig.6 The fundamental frequency of the propped cantilever nanoplate with respect to angular velocity for different nonlocal parameters and aspect ratios.

Fig.7 indicates the second frequency variation of the nanoplate with respect to the angular velocity. As can be seen, the second frequency decreases with increasing the aspect ratio. With increasing the angular velocity, the second frequency will be also increased. In addition, it is observed that the second frequency decreases with increasing the nonlocal parameter.

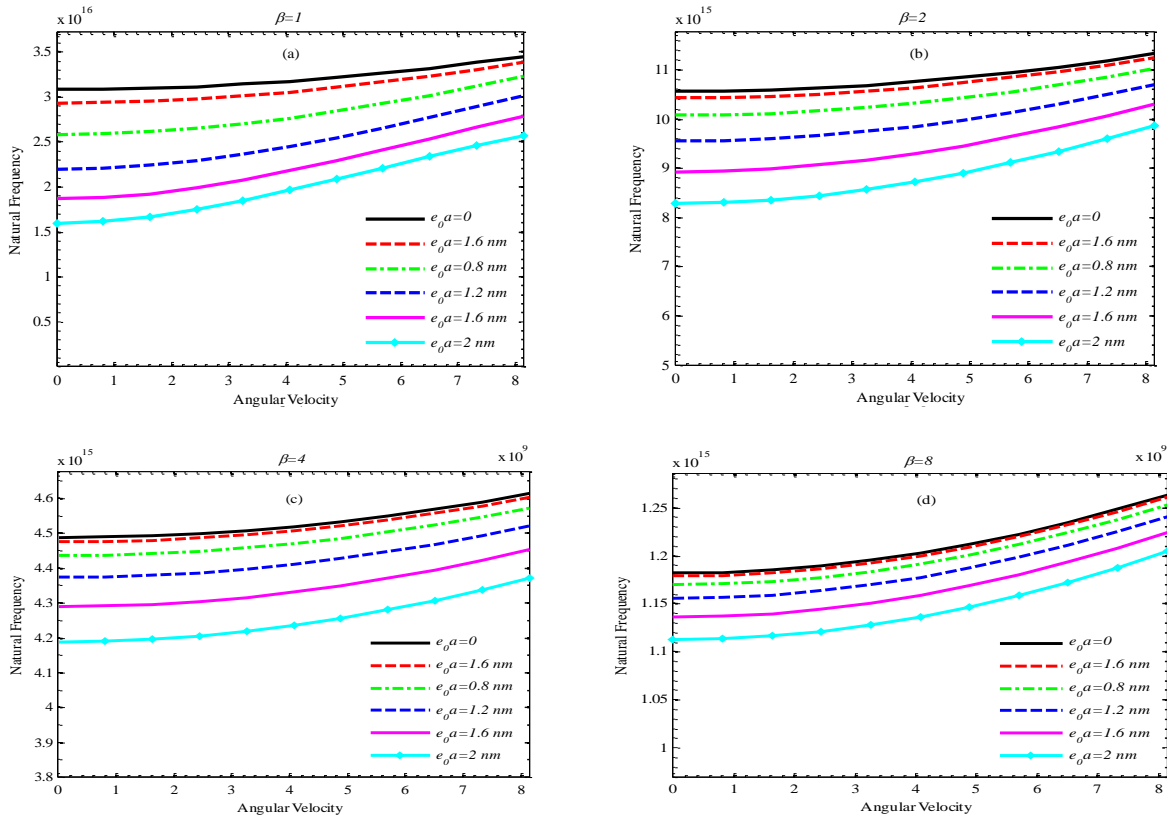
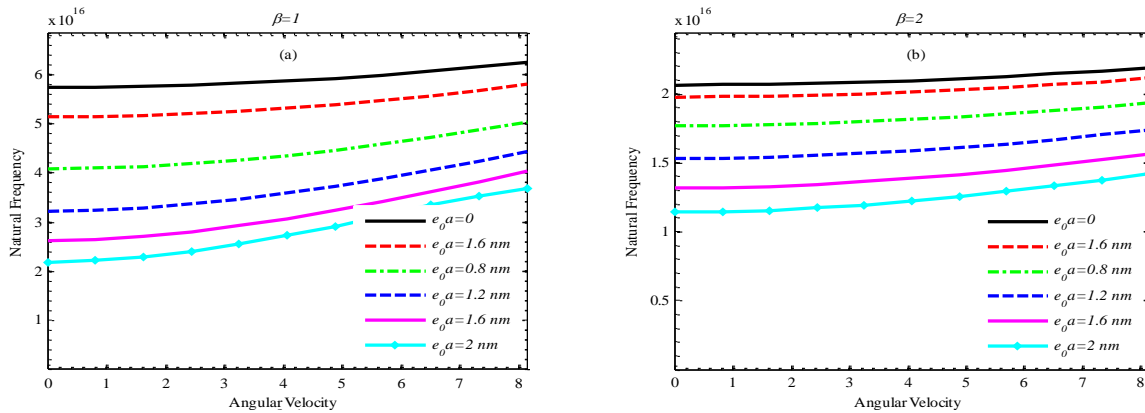


Fig.7 Second frequency of the propped cantilever nanoplate with respect to angular velocity, for different nonlocal parameters and aspect ratios.

The behavior of the third frequency of the nanoplate with respect to the angular velocity is shown in Fig.8. As can be seen, the third frequency decreases with increasing the aspect ratio. With increasing the angular velocity, the third frequency will be also increased. Lastly, increasing the nonlocal parameter results in decreasing the third natural frequency.



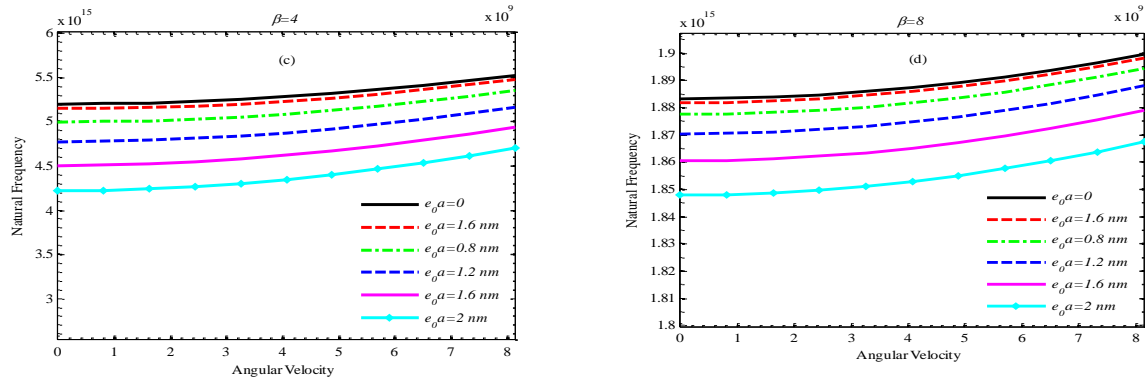


Fig.8
Third frequency of the propped cantilever nanoplate with respect to angular velocity, for different nonlocal parameters and aspect ratios.

Finally, the fourth frequency of the nanoplate with respect to the angular velocity is shown in Fig.9. As can be seen, with increasing the angular velocity, the fourth frequency will be increased. With increasing the nonlocal parameter, decreasing of the fourth frequency will be also observed.

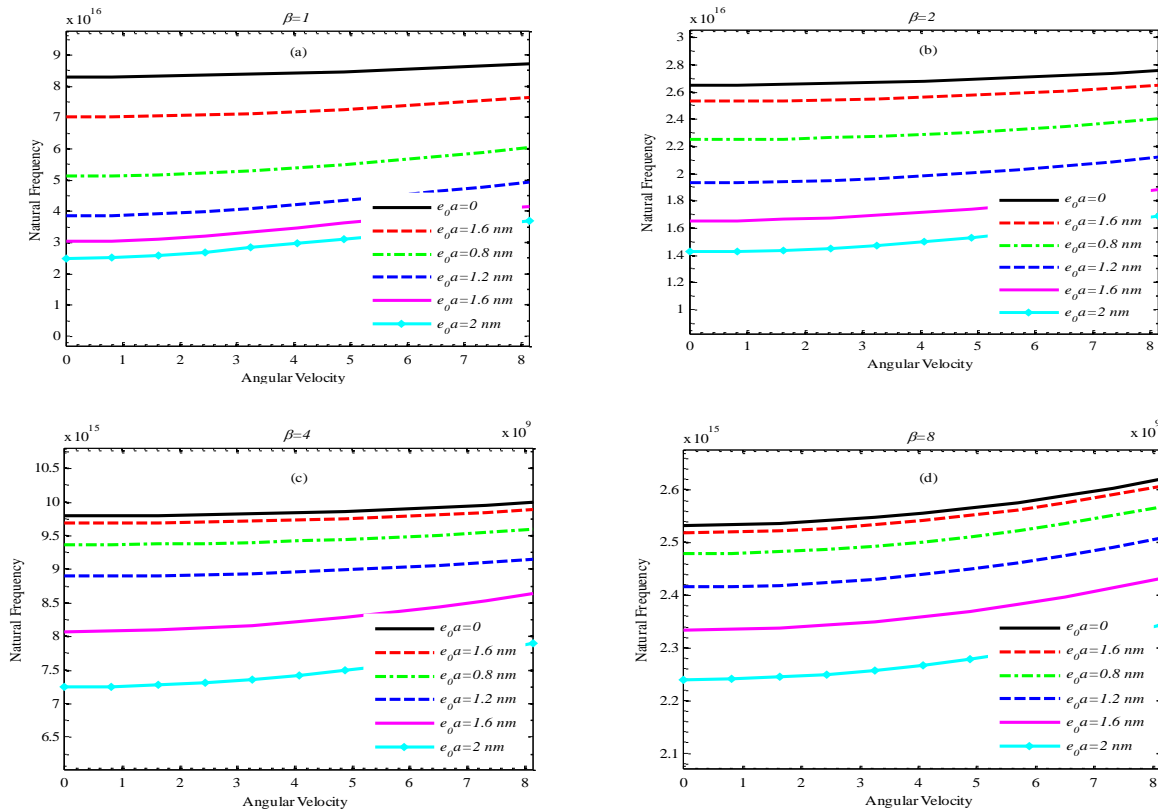


Fig.9
The Fourth frequency with respect to the angular velocity, nonlocal parameter and aspect ratio for the propped cantilever nanoplate.

5.3 Effect of hub radius

Fig.10 illustrates the effect of hub radius on fundamental frequency of the rotating nanoplate with cantilever boundary condition. The fundamental frequency is plotted with respect to the angular velocity and the nonlocal parameter for four hub radii: $r = 0, 1 \text{ nm}, 2 \text{ nm}$ and 4 nm .

The results show that for higher hub radius values, higher fundamental frequencies are expected. Figures also imply that in higher values of the nonlocal parameter, the fundamental frequency has a higher rate of change for a given change of the angular velocity or the hub radius.

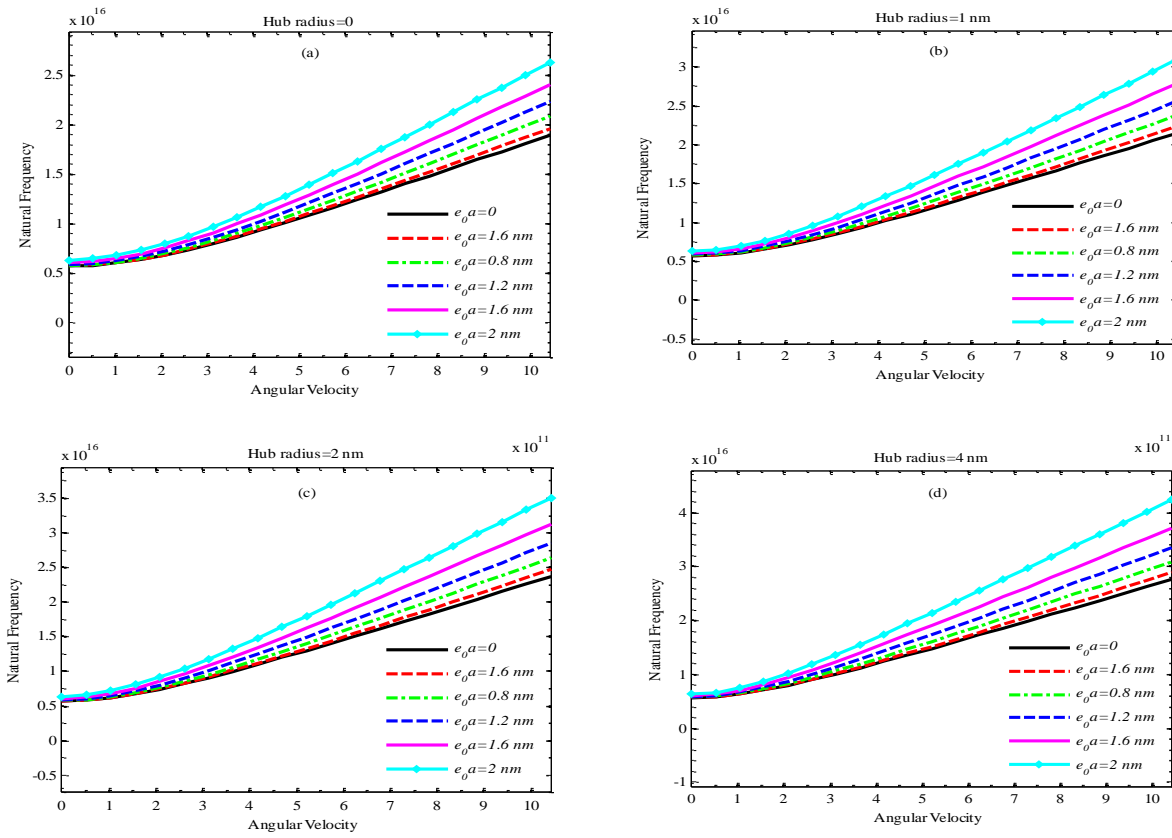
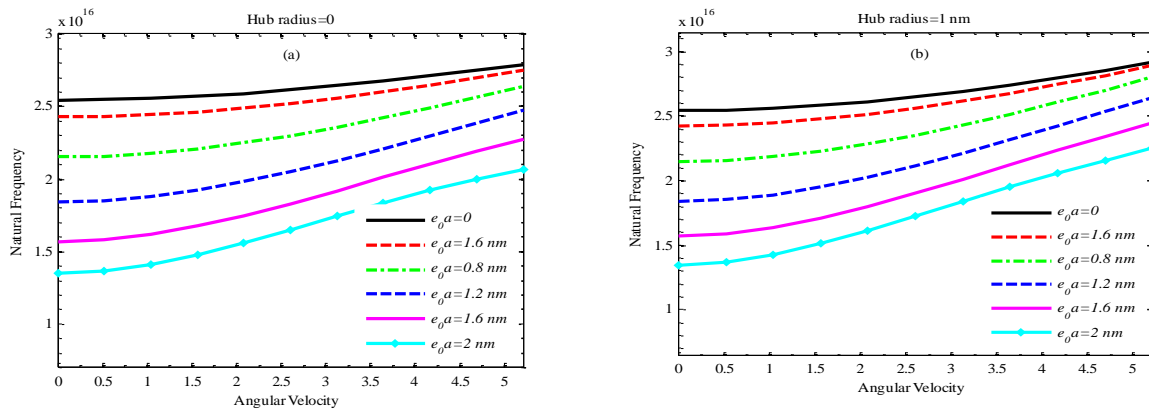


Fig.10 Effect of the hub radius on fundamental frequency of the rotating nanoplate for cantilever nanoplate.

The effect of hub radius on fundamental frequency of the rotating nanoplate with propped cantilever boundary condition is shown in Fig. 11. As results show, higher hub radius values result in higher fundamental frequencies. Figures also imply that in higher values of the nonlocal parameter, the fundamental frequency has a higher rate of change for a given change of the angular velocity or the hub radius.



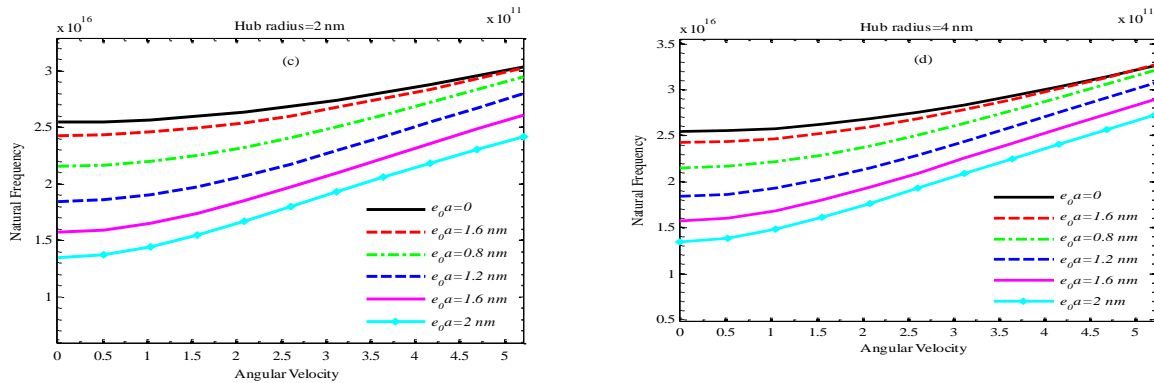


Fig.11

The Effect of hub radius on fundamental frequency of the rotating nanoplate for the propped cantilever nanoplate.

6 CONCLUSIONS

This paper has made the first attempt to study the vibration of the rotating nanoplate under variation of the axial force due to the rotation for two kinds of boundary conditions, i.e., the cantilever and the propped cantilever. Based on the nonlocal continuum mechanics and Hamilton's principle, the equations of motion were derived. Analytical expressions were obtained for the nondimensional frequency. DQ method as one of the efficient numerical methods was utilized to discrete the linear governing equations. The present model was validated by comparison with the available literatures. The obtained numerical results for the first four frequencies reveal that the vibration behavior of the nanoplate depends on angular velocity, hub radius and nonlocal parameter. Achieved conclusions are listed as follows. Frequency always increases with increasing the angular velocity or hub radius. In all cases the dependency of frequency on angular velocity also increases, with increasing the nonlocal parameter.

Fundamental frequency decreases with increasing the aspect ratio, but it is opposite for higher frequencies.

The behavior of frequency with respect to the nonlocal parameter depends on frequency number. Therefore, the first frequency increases with increasing the nonlocal parameter. For higher frequencies, this effect depends on rotational velocity. So, in low velocities, frequency is descending with respect to the nonlocal parameter which is different in high velocities. In higher frequencies, all involving parameters: rotational speed, frequency number and nonlocal parameter are correlated.

In this boundary condition, increasing the nonlocal parameter always results in decreasing all of the frequencies.

REFERENCES

- [1] Van Delden R. A., Ter Wiel M. K. J., Pollard M. M., Vicario J., Koumura N., Feringa B. L., 2005, Unidirectional molecular motor on a gold surface, *Nature* **437**(7063): 1337-1340.
- [2] Li J., Wang X., Zhao L., Gao X., Zhao Y., Zhou R., 2014, Rotation motion of designed nano-turbine, *Scientific Reports* **4**: 5846.
- [3] Fleck N., Muller G.M., Ashby M.F., Hutchinson J.W., 1994, Strain gradient plasticity: theory and experiment, *Acta Metallurgica et Materialia* **42**(2): 475-487.
- [4] Chong A. C. M., Yang F., Lam D. C. C., Tong P., 2001, Torsion and bending of micron-scaled structures, *Journal of Materials Research* **16**(04): 1052-1058.
- [5] Eringen A.C., 1983, On differential equations of nonlocal elasticity and solutions of screw dislocation and surface waves, *Journal of Applied Physics* **54**(9): 4703-4710.
- [6] Eringen A.C., 1972, Linear theory of nonlocal elasticity and dispersion of plane waves, *International Journal of Engineering Science* **10**(5): 425-435.
- [7] Chen M., 2013, Large deflection of a cantilever nanobeam under a vertical end load, *Applied Mechanics and Materials* **353**: 3387-3390.
- [8] Murmu T., Adhikari S., 2010, Scale-dependent vibration analysis of prestressed carbon nanotubes undergoing rotation, *Journal of Applied Physics* **108**(12): 123507-123514.
- [9] Narendar S., Gopalakrishnan S., 2011, Nonlocal wave propagation in rotating nanotube, *Results in Physics* **1**(1): 17-25.
- [10] Narendar, S., Mathematical modelling of rotating single-walled carbon nanotubes used in nanoscale rotational actuators, *Defence Science Journal* **61**(4): 317-324.

- [11] Akgoz B., Civalek O., 2012, Analysis of micro-sized beams for various boundary conditions based on the strain gradient elasticity theory, *Archive of Applied Mechanics* **82**(3): 423-443.
- [12] Challamel N., Wang C.M., 2008, The small length scale effect for a non-local cantilever beam: a paradox solved, *Nanotechnology* **19**(34): 345703.
- [13] Lim C., Li C., Yu J., 2009, The effects of stiffness strengthening nonlocal stress and axial tension on free vibration of cantilever nanobeams, *Interaction and Multiscale Mechanics: an International Journal* **1**(3): 223-233.
- [14] Narendar S., 2012, Differential quadrature based nonlocal flapwise bending vibration analysis of rotating nanotube with consideration of transverse shear deformation and rotary inertia, *Applied Mathematics and Computation* **219**(3): 1232-1243.
- [15] Pradhan S.C., Murmu T., 2010, Application of nonlocal elasticity and DQM in the flapwise bending vibration of a rotating nanocantilever, *Physica E: Low-dimensional Systems and Nanostructures* **42**(7): 1944-1949.
- [16] Aranda-Ruiz J., Loya J., Fernández-Sáez J., 2012, Bending vibrations of rotating nonuniform nanocantilevers using the Eringen nonlocal elasticity theory, *Composite Structures* **94**(9): 2990-3001.
- [17] Ghadiri M., Hosseini S., Shafiei N., 2016, A power series for vibration of a rotating nanobeam with considering thermal effect, *Mechanics of Advanced Materials and Structures* **23**(12): 1414-1420.
- [18] Ghadiri M., Shafiei N., 2016, Nonlinear bending vibration of a rotating nanobeam based on nonlocal Eringen's theory using differential quadrature method, *Microsystem Technologies* **22**(12): 2853-2867.
- [19] Kiani K., 2011, Nonlocal continuum-based modeling of a nanoplate subjected to a moving nanoparticle, *Part I: Theoretical Formulations*, *Physica E: Low-dimensional Systems and Nanostructures* **44**(1): 229-248.
- [20] Kiani K., 2011, Nonlocal continuum-based modeling of a nanoplate subjected to a moving nanoparticle, *Part II: Parametric Studies*, *Physica E: Low-dimensional Systems and Nanostructures* **44**(1): 249-269.
- [21] Kiani K., 2011, Small-scale effect on the vibration of thin nanoplates subjected to a moving nanoparticle via nonlocal continuum theory, *Journal of Sound and Vibration* **330**(20): 4896-4914.
- [22] Kiani K., 2013, Vibrations of biaxially tensioned-embedded nanoplates for nanoparticle delivery, *Indian Journal of Science and Technology* **6**(7): 4894-4902.
- [23] Salehipour H., Nahvi H., Shahidi A., 2015, Exact analytical solution for free vibration of functionally graded micro/nanoplates via three-dimensional nonlocal elasticity, *Physica E: Low-dimensional Systems and Nanostructures* **66**: 350-358.
- [24] Ansari R., Shahabodini A., Shojaei M.F., 2016, Nonlocal three-dimensional theory of elasticity with application to free vibration of functionally graded nanoplates on elastic foundations, *Physica E: Low-dimensional Systems and Nanostructures* **76**: 70-81.
- [25] Wang C., Reddy J.N., Lee K., 2000, *Shear Deformable Beams and Plates: Relationships with Classical Solutions*, Elsevier.
- [26] Reddy J.N., El-Borgi S., 2014, Eringen's nonlocal theories of beams accounting for moderate rotations, *International Journal of Engineering Science* **82**(0):159-177.
- [27] Wang J.S., Shaw D., Mahrenholtz O., 1987, Vibration of rotating rectangular plates, *Journal of Sound and Vibration* **112**(3): 455-468.
- [28] Shu C., Richards B.E., 1992, Application of generalized differential quadrature to solve two-dimensional incompressible Navier-Stokes equations, *International Journal for Numerical Methods in Fluids* **15**(7): 791-798.
- [29] Pradhan S.C., Phadikar J.K., 2009, Nonlocal elasticity theory for vibration of nanoplates, *Journal of Sound and Vibration* **325**(1-2): 206-223.
- [30] Mohammadi M., Moradi A., Ghayour M., Farajpour A., 2014, Exact solution for thermo-mechanical vibration of orthotropic mono-layer graphene sheet embedded in an elastic medium, *Latin American Journal of Solids and Structures* **11**: 437-458.
- [31] Shen Z. B., Tang H.L., Daokui L., Tang G.J., 2012, Vibration of single-layered graphene sheet-based nanomechanical sensor via nonlocal Kirchhoff plate theory, *Computational Materials Science* **61**(0):200-205.
- [32] Ansari R., Rajabiehfarid R., Arash B., 2010, Nonlocal finite element model for vibrations of embedded multi-layered graphene sheets, *Computational Materials Science* **49**(4): 831-838.